Title

Visual feedback alters force control and functional activity in the visuomotor network after stroke

Authors

Archer, Derek B

Kang, Nyeonju

Misra, Gaurav

et al.

Publication Date

2018

DOI

10.1016/j.nicl.2017.11.012

NeuroImage: Clinical 17 (2018) 505–517

Contents lists available at ScienceDirect

NeuroImage: Clinical

journal homepage: www.elsevier.com/locate/ynicl

Visual feedback alters force control and functional activity in the visuomotor network after stroke

Derek B. Archer[a], Nyeonju Kang[b], Gaurav Misra[a], Shannon Marble[a], Carolynn Patten[c], Stephen A. Coombes[a,*]

[a] Laboratory for Rehabilitation Neuroscience, Department of Applied Physiology and Kinesiology, University of Florida, Gainesville, FL, United States
[b] Division of Sport Science, Incheon National University, Incheon, South Korea
[c] Neural Control of Movement Lab, Department of Physical Therapy, University of Florida and Malcolm-Randall VA Medical Center, Gainesville, FL, United States

ARTICLE INFO

Keywords:
Stroke
Force control
Visual feedback
fMRI
Visuomotor network
Ipsilateral M1

ABSTRACT

Modulating visual feedback may be a viable option to improve motor function after stroke, but the neurophysiological basis for this improvement is not clear. Visual gain can be manipulated by increasing or decreasing the spatial amplitude of an error signal. Here, we combined a unilateral visually guided grip force task with functional MRI to understand how changes in the gain of visual feedback alter brain activity in the chronic phase after stroke. Analyses focused on brain activation when force was produced by the most impaired hand of the stroke group as compared to the non-dominant hand of the control group. Our experiment produced three novel results. First, gain-related improvements in force control were associated with an increase in activity in many regions within the visuomotor network in both the stroke and control groups. These regions include the extrastriate visual cortex, inferior parietal lobule, ventral premotor cortex, cerebellum, and supplementary motor area. Second, the stroke group showed gain-related increases in activity in additional regions of lobules VI and VIIb of the ipsilateral cerebellum. Third, relative to the control group, the stroke group showed increased activity in the ipsilateral primary motor cortex, and activity in this region did not vary as a function of visual feedback gain. The visuomotor network, cerebellum, and ipsilateral primary motor cortex have each been targeted in rehabilitation interventions after stroke. Our observations provide new insight into the role these regions play in processing visual gain during a precisely controlled visuomotor task in the chronic phase after stroke.

1. Introduction

Stroke often causes impairments in visually-guided motor control (Chang et al., 2013; Li et al., 2014; Lindberg et al., 2012; Lodha et al., 2010). Force production by individuals in the chronic phase after stroke reveals greater error and greater variability when using the impaired hand (Kang and Cauraugh, 2015b; Lodha et al., 2010). Dependence on visual feedback increases after stroke (Bonan et al., 2004a; Kang and Cauraugh, 2015a; Westerveld et al., 2013), with evidence suggesting that manipulating visual feedback can enhance motor function (Brewer et al., 2005; Brewer et al., 2008; Patton et al., 2006; Tunik et al., 2013) by decreasing motor error and motor variability after stroke (Archer et al., 2016). Although these findings converge to suggest that modulating visual feedback is a viable option to improve motor output (Carter et al., 2010; Tunik et al., 2013), the neurophysiological basis for this improvement has not been examined. Understanding how visual feedback engages the brain in the chronic phase after stroke may be useful when designing visual displays for rehabilitation interventions for individuals in the chronic phase after stroke. Here, we use functional magnetic resonance imaging (fMRI) to examine how brain activity in the visuomotor network changes in chronic stroke patients when visual gain is parametrically increased during a grip force task.

In healthy individuals, using visual gain to engage error correction processes relies on an integrated network of brain areas that include the primary motor cortex (M1), premotor cortex, inferior and posterior parietal lobe, extrastriate visual cortex, and cerebellum (Bagce et al., 2012; Coombes et al., 2010). These brain regions are essential components of the visuomotor network (Grafton et al., 1992), and disruptions to this network lead to deficits in visuomotor error correction (Della-Maggiore et al., 2004; Desmurget et al., 1999; Lee and van Donkelaar, 2006; Van Donkelaar et al., 2000). It is well established that stroke leads to changes in activation of the visuomotor motor system. For instance, reductions in functional activity have been demonstrated in M1 contralateral to the impaired hand, whereas increases in

* Corresponding author at: University of Florida, Laboratory for Rehabilitation Neuroscience, Department of Applied Physiology and Kinesiology, PO Box 118206, United States.
E-mail address: scoombes@ufl.edu (S.A. Coombes).

https://doi.org/10.1016/j.nicl.2017.11.012
Received 1 June 2017; Received in revised form 9 November 2017; Accepted 13 November 2017
Available online 14 November 2017

functional activity have been shown in M1 ipsilateral to the impaired hand, bilateral premotor areas, and parietal cortex (Chollet et al., 1991; Cramer et al., 1997; Loubinoux et al., 2007; Marshall et al., 2009; Rehme et al., 2012; Ward et al., 2003b, 2004; Weiller et al., 1993). It is important to note, however, that increases in activity within these sub-regions of the motor network are time-dependent and are most prominent in acute stroke before progressively decreasing across time (Bonstrup et al., 2015; Ward et al., 2003b). Indeed, relative increases in activity in contralateral M1, and decreases in activity in secondary motor areas track well with functional recovery after stroke (Buetefisch, 2015; Favre et al., 2014), with recent evidence showing that this time-dependent change in activity is not related to an increase in effort in the acute phase (Bonstrup et al., 2015).

Well-controlled visually guided motor paradigms have been used to assess motor system activation after stroke (Bestmann et al., 2010; Bonstrup et al., 2015; Nowak et al., 2003; Ward et al., 2003b), but few studies have scaled the parameters of visual feedback. The studies that have assessed brain function while modulating the properties of visual feedback have done so using virtual reality paradigms (Bagce et al., 2012; Tunik et al., 2013). For instance, scaling down virtual reality feedback relative to actual finger movement led to larger finger movements in the impaired hand which were associated with increased activity in contralateral M1 in the lesioned hemisphere. These findings are consistent with evidence in healthy adults which show that increasing visual gain during a visuomotor grip force task also leads to an increase in contralateral M1 activity, even in the absence of a change in force amplitude (Coombes et al., 2010). Together, these findings suggest that manipulating visual feedback while keeping force amplitude constant may be a viable option for engaging M1 contralateral to the impaired hand after stroke. In the current study, we test this hypothesis by using fMRI to assay brain activity while participants completed a visually guided unilateral grip force paradigm at three levels of visual gain. We hypothesized that force error and variability would decrease with an increase in visual gain after stroke, and that this gain-related change in force control would be associated with increased functional activity in the visuomotor network including M1 contralateral to the impaired hand.

2. Methods

2.1. Subjects

Fifteen individuals in the chronic phase after stroke and fifteen healthy controls participated in this study. Table 1 shows group demographics and relevant clinical information. We confirmed that healthy controls were matched to the post-stroke individuals for age and sex ($P > 0.05$). Individuals with stroke who met the following inclusion criteria were recruited: (1) at least six months following a single ischemic stroke affecting motor function in the contralateral hand, (2) able to apply force to a force transducer in the pinch grip configuration, (3) intact sensation to light touch in the contralateral hand, and (4) able to provide informed consent. Before the testing, each subject read and signed informed consent, which was approved by Institutional Review Board of the University of Florida and was in accord with the Declaration of Helsinki.

2.2. Clinical evaluations

Upper-extremity motor function for persons with stroke was assessed using the upper extremity section of the Fugl-Meyer Assessment (FMA) (Fugl-Meyer et al., 1975; Gladstone et al., 2002). Hypertonicity was measured using the Modified Ashworth Scale (Bohannon and Smith, 1987; Haas et al., 1996). Hemiparetic severity (mean FMA 44.13 out of 66 points) and stroke chronicity (mean 8.15 years) indicated a wide range of stroke-related upper-extremity impairments. Using the Mini-Mental State Examination (Folstein et al., 1975), we screened cognitive function for each individual. All stroke subjects self-reported pre-morbid right hand dominance and all controls self-reported right hand dominance. Lesion characteristics of the stroke subjects were evaluated by hand-drawing the lesion in standard space. The volume and center of mass were calculated for each individual's lesion and are shown in Table 2. We then calculated the lesion conjunction with each of the six white matter tracts available in the Sensorimotor Area Tract Template (S-MATT) (Archer et al., 2017), and the results from this analysis are shown in Fig. 1.

2.3. MRI acquisition

Magnetic resonance images were collected using a 32 channel head coil inside a Phillips 3 Tesla magnetic resonance scanner (Achieva, Best, the Netherlands). T_1-weighted images (resolution: 1 mm isotropic, repetition time: TR = 6.8 ms, echo time: TE = 3.3 ms, flip angle = 8°, field of view = 240 × 240 mm, and acquisition matrix = 240 × 240) were acquired in 170 contiguous axial slices. Functional data were acquired in 46 contiguous axial slices using a single-shot gradient echo-planar imaging pulse sequence (resolution: 3 mm isotropic, TR = 2500 ms, TE = 30 ms, flip angle = 80°, field of view = 240 mm^2, and acquisition matrix = 80 × 80). Each functional MRI scan lasted 4 min and 30 s. Subjects wore ear plugs during the session to minimize discomfort because of scanner noise. Small

Table 1
Group demographics and relevant clinical information.

Subject	Age (yrs)	Gender	Time since stroke (yrs)	Stroke location	Affected hemisphere	FMA motor score	FMA sensation	MAS median	MMSE
1	63	M	12.4	C/SC	L	49	12	1	27
2	52	M	0.73	SC	L	45	8	1	30
3	79	M	10.21	C/SC	L	62	9	0	29
4	76	F	2.67	SC	L	64	12	0	30
5	56	M	24.45	SC	L	30	7	0	24
6	77	M	12.48	C	L	10	12	0	27
7	59	M	17.65	C/SC	L	51	12	0	27
8	58	M	1.29	SC	L	62	12	0	29
9	73	M	4.94	C	L	58	12	0	30
10	64	M	9.66	C	L	65	12	0	30
11	50	F	1.65	SC	L	61	9	0	27
12	56	M	4.3	C/SC	R	30	4	0	30
13	57	M	9.61	C	R	26	10	1	30
14	31	M	5.53	C	R	19	10	3	29.5
15	75	F	4.67	SC	R	30	12	1	27
Mean	61.73 ± 12.90	12M/3F	8.15 ± 6.65		11L/4R	44.13 ± 18.40	10.20 ± 2.43	0.46 ± 0.83	28.43 ± 1.82
Control	58.20 ± 6.82	10M/5F				n/a	n/a	n/a	29.93 ± 0.26

Abbreviations: yrs., years; M, male; F, female; C, cortical; SC, subcortical; L, left; R, right; FMA, Fugl-Meyer Assessment; MAS, Modified Ashworth Scale; MMSE, Mini-Mental State Exam.

Table 2
Lesion volumes and centers of mass.

Subject	Lesion volume (mm^3)	Center of mass		
		x	y	z
1	15,809	− 35.22	11.67	22.41
2	148	− 25.65	15.66	21.17
3	2089	− 36.54	31.39	− 6.06
4	313	− 24.51	− 1.70	0.59
5	43	− 23.89	8.56	− 5.07
6	1561	− 37.18	15.40	24.97
7	5093	− 38.07	3.82	15.24
8	125	− 24.03	10.72	− 3.54
9	782	− 33.10	12.61	28.37
10	7195	− 35.92	− 3.63	13.65
11	348	− 27.57	34.09	30.71
12	16,378	41.73	8.34	25.54
13	7657	43.34	11.38	33.05
14	671	26.33	16.52	57.23
15	913	23.20	14.57	8.64

cushions were placed in the head coil around the subject's head to minimize head motion.

2.4. Force data acquisition

Participants laid in supine, with their forearms resting on their lower trunk and one force transducer held in each hand at all times. Participants produced force against a custom fiber-optic force transducer with a resolution of 0.025 N (Neuroimaging Solutions, Gainesville, FL). The force signals were transmitted via fiber-optic cable to a SM130 Optical Sensing Interrogator (Micron Optics, Atlanta, Georgia). The interrogator digitized the analog force data at 125 Hz. Using a customized program written in LabVIEW (National Instruments, Austin, TX), we collected the force data. Online visual feedback of force output was displayed to the participants at a refresh rate of 60 Hz. Force data were low-pass filtered before analysis (Butterworth, 20 Hz 4th-order dual-pass).

2.5. Force task

We measured each participant's maximum voluntary contraction (MVC) for each hand during a practice session. Over three consecutive MVC trials, participants tried to sustain a maximum force contraction for 5 s. We provided a 60-second period of rest between trials. Average force during each sustained maximum force contraction was calculated and the mean of the three trials was carried forward as the participant's MVC value.

We collected functional MRI data while each participant produced and tried to maintain force to a target force level of 15% of their MVC by gripping the force transducer between their thumb and index finger. Blocks of trials were performed unimanually with the impaired and unimpaired hand for patients with stroke, and the dominant and non-dominant hand for healthy controls. For all analyses, the dominant hand in controls was compared to the unimpaired hand in the stroke group. The non-dominant hand in controls was compared to the impaired hand in the stroke group. Our approach is consistent with prior work (Archer et al., 2016; Lodha et al., 2012a; Lodha et al., 2010; Naik et al., 2011). Three unimanual tasks were completed by each hand: low visual gain, medium visual gain, and high visual gain. Thus, participants completed a total of six tasks (two hands × three gain levels) while lying in the MRI scanner.

Each task involved two conditions: Rest and Force. Two bars were displayed during the task. A white target bar represented the target force level, which was set at 15% of each individual's MVC. A red/green bar shows either rest or the amount of force produced by the subject. During the Rest condition, participants were instructed to fixate on the red bar. When the bar turned green, participants started producing isometric force and the bar fluctuated in real-time to reflect the amount of force being produced. We instructed participants to be as accurate as possible and cover the white target bar with the green force bar. The force bar represented the force produced by a single transducer during each unimanual task. The transducer in the other hand was used to assess force production in the passive hand. Rest and force conditions each lasted 30 s and were alternated within each scan. Each scan began and ended with a rest period. Blocks within each scan followed the same sequence and were displayed on the visual display. The duration of each scan was 4 min and 30 s in total. Visual gain was manipulated between scans.

2.6. Visual gain

We manipulated visual feedback between tasks by changing the visual gain on the visual display seen by the participants. Our paradigm first calculated the difference between the amount of force produced by the subject and the target force. This difference was then multiplied by a visual gain factor (low, medium, and high), which changed the spatial amplitude of visual feedback by altering the height of force fluctuations on the visual display using the following formula:

$$Cursor\ Position = (F_p - F_t)^{*}G + F_t \quad (1)$$

in which F_p is the force produced by the subject, F_t is the target force, and G is the gain level used to manipulate the spatial amplitude of visual feedback.

The visual gain level (G) can be altered by modifying two different

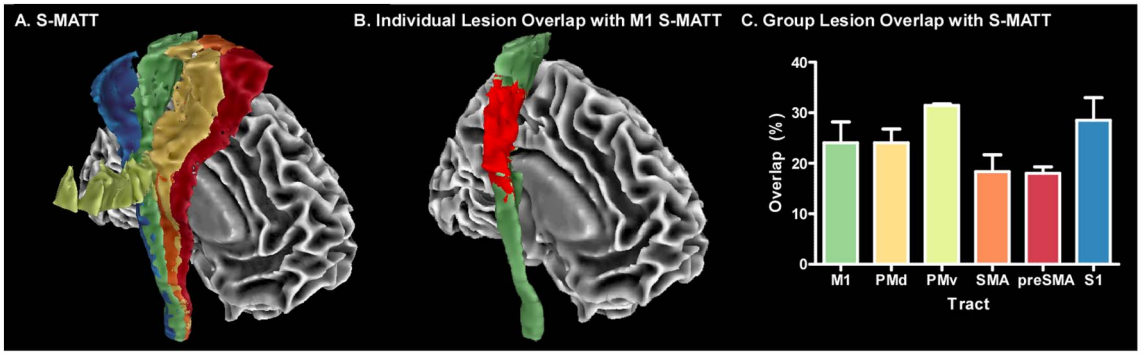

Fig. 1. Lesion overlap with the sensorimotor area tract template (S-MATT).
The S-MATT (A) is comprised of six separate sensorimotor tracts descending from the primary motor cortex (M1), dorsal premotor cortex (PMd), ventral premotor cortex (PMv), supplementary motor area (SMA), pre-supplementary motor area (preSMA), and somatosensory cortex (S1). Each individual's lesion was overlaid on top of each tract within the S-MATT to quantify lesion overlap within the tract (see example in B). The mean lesion overlap for each tract is shown in C, with each column representing the group average. Error bars represent ± SEM.

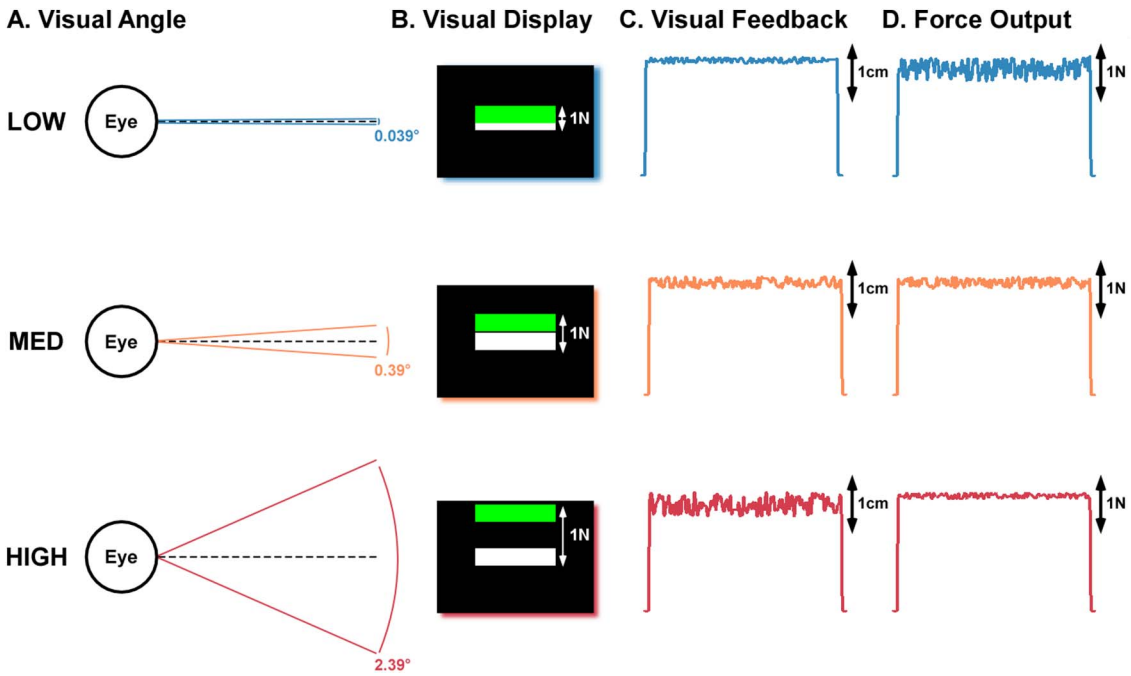

Fig. 2. Visual gain manipulation.
The gain of the visual feedback was altered between functional MRI scans which led to a change in the visual angle of the feedback (A). At larger visual angles, the spatial amplitude of the visual feedback is increased even though the distance in absolute force (N) between the target bar and the force bar remains constant (e.g., 1N) (B). Since visual angle is increased from low to medium to high, there is an increase in the spatial amplitude of the visual feedback (C), which is typically associated with a reduction in force output variability (D).

variables: (1) distance from the visual display, or (2) changing the height of the force fluctuations provided to the participant on the visual display. We have previously shown that performance error approaches an asymptote at approximately 0.5°. However, we have also demonstrated that changes in activity in the visuomotor system are evident above and below this 0.5° asymptote (Coombes et al., 2010). Therefore, we used three different visual gain levels (0.039°, 0.39°, and 2.39°). Values were chosen so that one was well below the 0.5° asymptote, one was near the asymptote, and one was well above the asymptote. Fig. 2 shows a cartoon to explain the visual gain manipulation. At the low visual gain level (Fig. 2A), a 1 N difference between the target bar and the force bar is represented by a small displacement on the screen such that the green bar and white bar are close to each other (Fig. 2B). By attenuating the visual error, there are very small fluctuations in the visual feedback viewed by the subject, and so the range of the spatial amplitude of the visual feedback on the screen is reduced (Fig. 2C), which leads to greater force variability and greater force error (Fig. 2D). At the medium gain level, the visual angle is increased, the error is magnified, and a difference of 1 N of force between the green bar and white bar is represented by a larger spatial amplitude. The spatial amplitude of the visual feedback is therefore increased (see progression from top to bottom row in Fig. 2C) and corresponds with a decrease in force variability and force error (see progression in Fig. 2D). This pattern is further increased at the high visual gain level, where visual angle is increased to 2.39°. To control for potential order effects, both hand order and visual gain order for each hand were counterbalanced across subjects.

2.7. Force data analysis

Force data were analyzed using custom algorithms in LabVIEW. Three outcome measures for force data were: (a) mean force amplitude, (b) mean force error (root-mean-square error), and (c) mean force variability (standard deviation). Force measures were calculated using the middle 18 s of each contraction. We excluded the beginning (first 7 s) and ending (last 5 s) segments of force production as they are likely independent of visuomotor processing (Coombes et al., 2010; Lodha et al., 2012a; Lodha et al., 2012b; Naik et al., 2011). All force measures were calculated separately for each hand at each gain level. For each outcome measure, two-way mixed model 2 × 3 (Group: stroke and control × Gain: low, medium, and high) ANOVAs with repeated measures on the last factor were used. When assumptions of sphericity were violated, we used Greenhouse-Geisser's conservative degrees of freedom adjustment. For post-hoc analyses, we used Bonferroni's pairwise comparisons. All statistical tests on force data were performed using IBM SPSS Statistics 22 (IBM, USA) with an alpha level set at 0.05.

2.8. Imaging data analysis software

Imaging data were analyzed with AFNI software (Analysis of Functional NeuroImages; National Institutes of Health, Bethesda, MD), SPM8 software, SUIT toolbox of SPM8, and custom UNIX shell scripts. Based on the different behavioral findings between stroke and control groups with an increased visual gain, we focused on imaging data during the task executed by the impaired hand in the stroke group and non-dominant hand in the control group. We used AFNI software to compute whole-brain statistical maps. Cerebellum-specific fine-tuning of the statistical maps was performed with SPM8 and SUIT. With conventional normalization techniques, priority is given to the cortex; therefore, alignment of the cerebellum is more variable between subjects. For this reason, we used the SUIT toolbox of SPM8, which is specifically designed to precisely align the cerebella of subjects to a cerebellum template (Diedrichsen, 2006).

2.9. Individual subject analysis

2.9.1. Preprocessing

Four functional volumes were collected prior to the start of the experiment to allow for magnetization to stabilize; these volumes were discarded prior to analysis. Remaining volumes were slice-acquisition-dependent slice-time corrected. The anatomical image was then skull stripped using 3dSkullStrip in AFNI. The functional volumes were

registered to a base volume via rigid body rotations and aligned with the anatomical image in a single transformation, therefore avoiding repeated image resampling. For the whole brain analysis, the functional volumes were also warped into MNI space and smoothed with a 4 mm full-width-half-maximum Gaussian kernel to increase the signal-to-noise ratio. For the cerebellum analysis, warping to MNI space and smoothing occurred later (detailed below). The blood-oxygen-level dependent (BOLD) signal in each voxel at each time point was then scaled by the mean of its respective time series to normalize the data.

The BOLD signals during the Force and Rest period were modeled separately by boxcar regressors convolved with the hemodynamic response function for each task. The head motion parameters (6 total: 3 rotations and 3 translations) calculated during the registration step were included in the general linear model as regressors-of-no-interest. Head motion between adjacent volumes which was > 1 mm resulted in the exclusion of both volumes from the regression analysis. Within both groups, a large number of adjacent volumes remained after excluding for head motion for all six tasks (stroke average: 96.93 ± 4.80%; stroke minimum: 76.5%; control average: 99.35 ± 1.39%; control minimum: 94.1%). Whole-brain beta-coefficient maps were obtained for each experimental condition from the general linear model implemented in AFNI.

2.9.2. SUIT normalization

Skull-stripped anatomical images were aligned to the SPM8 white-matter template. The transformation matrix used for this alignment was applied to the beta-coefficient maps obtained from AFNI, thus keeping the beta-value maps consistent with the anatomical image. Next, the cerebellum was isolated from the whole brain anatomical image using the SUIT toolbox of SPM8. A mask was derived from the isolated cerebellum and was used to isolate the cerebellar region from the whole brain beta-coefficient maps. The isolated anatomical image of the cerebellum was then normalized to the SUIT template, which is in MNI space. The transformation matrix used for this normalization was saved and applied to the isolated cerebellar beta-value maps to keep them consistent with the anatomical image. The beta-coefficient maps were smoothed with a 2 mm full-width-at-half-max Gaussian kernel in order to improve the signal-to-noise ratio. The cerebellar beta-coefficient maps from all subjects were taken to the group level for further analysis, which was conducted using the same pipeline as the cortical data.

2.10. Group level analysis

To investigate the effect of visual gain and stroke on brain function, a two-way mixed model ANOVA was conducted (AFNI's 3dANOVA program) with group (stroke, control) as a between-subjects factor and visual gain (low, medium, and high) as a within-subjects factor. Separate ANOVAs were conducted for the whole brain beta-coefficient maps and the beta-coefficient maps isolated and warped to the cerebellum. Both group and visual gain were treated as fixed effects, and subjects were treated as random effects. Familywise error rate (FWER) in the group-level statistical maps was maintained below 0.05 by rejecting voxels with P-values > 0.005 and clusters with volume < 216 mm^3 for the cortex and < 162mm^3 for the cerebellum. The P-value threshold and cluster-extent threshold required to maintain the required FWER were selected by using AFNI's 3dClustSim program. First, we identified all voxels which showed significant increases in activity ($P < 0.05$) for both groups at each gain level, and then created a conjunction of all six maps. The inputs into 3dClustSim included the mean smoothness of the residual datasets and the conjunction mask of all six maps. Monte Carlo simulations of noise datasets were created within these masks. Then, a frequency distribution of noise-cluster sizes was created and the program calculated the appropriate P-value and cluster extent required to control the FWER at 0.05. Activation clusters were labeled using a combination of the cytoarchitecture probabilistic map (Desikan et al., 2006), the Human Motor Area Template (HMAT) (Mayka et al., 2006), and the automated anatomical labeling atlas for the cortex (Tzourio-Mazoyer et al., 2002). The probabilistic MRI atlas of the human cerebellum was used to label the SUIT-aligned cerebellar data (Diedrichsen et al., 2009; Schmahmann et al., 1999).

3. Results

3.1. MVC

The average MVC of the impaired hand for the stroke group (41.64 ± 6.19 N) was significantly less [$t(28) = 3.05$; $P < 0.01$] than the average MVC of the non-dominant hand for the control group (70.00 ± 6.94 N). The average MVC of the unimpaired hand for the stroke group (69.91 ± 4.56 N) was not significantly different than the average MVC of the dominant hand for the control group (75.43 ± 7.32 N).

3.2. Force data analysis

3.2.1. Force amplitude

Mean force amplitude in % MVC produced by the unimpaired/dominant and impaired/non-dominant hands is shown for both groups in Fig. 3A and D, respectively. Mean force across all conditions and groups ranged from 13.39–14.98%MVC. Consistent with the data shown in Fig. 3A, a group × gain ANOVA model to assess mean force amplitude produced by the unimpaired/dominant hand revealed no significant effect of group [$F(1, 28) = 0.28$; $P = 0.60$], gain [$F(1.01, 28.15) = 0.52$; $P = 0.479$], or group × gain interaction [$F(1.01, 28.15) = 0.21$; $P = 0.652$]. As shown in Fig. 3D, mean force amplitude produced by the impaired/non-dominant hand at the low gain level for the stroke group was 13.39%MVC (red triangles) and 14.44%MVC for the control group (green squares), respectively. At the medium and high gain levels, mean force amplitude was within 1% of the target force level for both groups. Similar to findings in the unimpaired/dominant hand, the two-way ANOVA of mean force amplitude for the impaired/non-dominant hand revealed no significant effect of gain [$F(1.05, 29.37) = 1.21$; $P = 0.283$], group [$F(1,28) = 1.21$; $P = 0.281$], or group × gain interaction [$F(1.05, 29.37) = 0.27$; $P = 0.618$].

3.2.2. Force error

Mean force error produced by the unimpaired/dominant and impaired/non-dominant hands are shown for both groups in Fig. 3B and E, respectively. A two-way (group × gain: 2 × 3) ANOVA on the unimpaired/dominant hand revealed a main effect of gain [$F(1.017, 28.47) = 46.82$; $P < 0.001$; $\eta^2 = 0.63$], showing a reduction in error with an increase in visual gain (low > medium > high; all adjusted $P's < 0.001$). There was no significant effect of group [$F(1,28) = 0.001$; $P = 0.974$], and no group × gain interaction [$F(1.017, 28.47) = 0.12$; $P = 0.74$].

Fig. 3E shows mean force error for the stroke and control group at each level of visual gain for the impaired/non-dominant hand. A group × gain ANOVA on the impaired/non-dominant hand revealed a main effect of gain [$F(1.06, 29.64) = 34.42$; $P < 0.001$; $\eta^2 = 0.55$], and a main effect of group [$F(1, 28) = 11.04$; $P = 0.002$; $\eta^2 = 0.28$]. However, main effects were superseded by a significant group × gain interaction [$F(1.06, 29.64) = 6.63$; $P = 0.014$; $\eta^2 = 0.19$]. Post-hoc analyses found that stroke individuals produced more force error than controls at each of the three gain levels (all adjusted $P's < 0.01$). Difference in force error between the stroke and control groups was approximately 21%MVC at the low visual gain, with the magnitude of the difference attenuated at medium gain (approximate 6%MVC) and high gain (approximate 3%MVC). Moreover, mean force error in the stroke (low > medium > high; all adjusted $P's < 0.01$) and control (low > medium > high; all adjusted $P's < 0.05$) groups was significantly reduced with an increase in the level of visual gain.

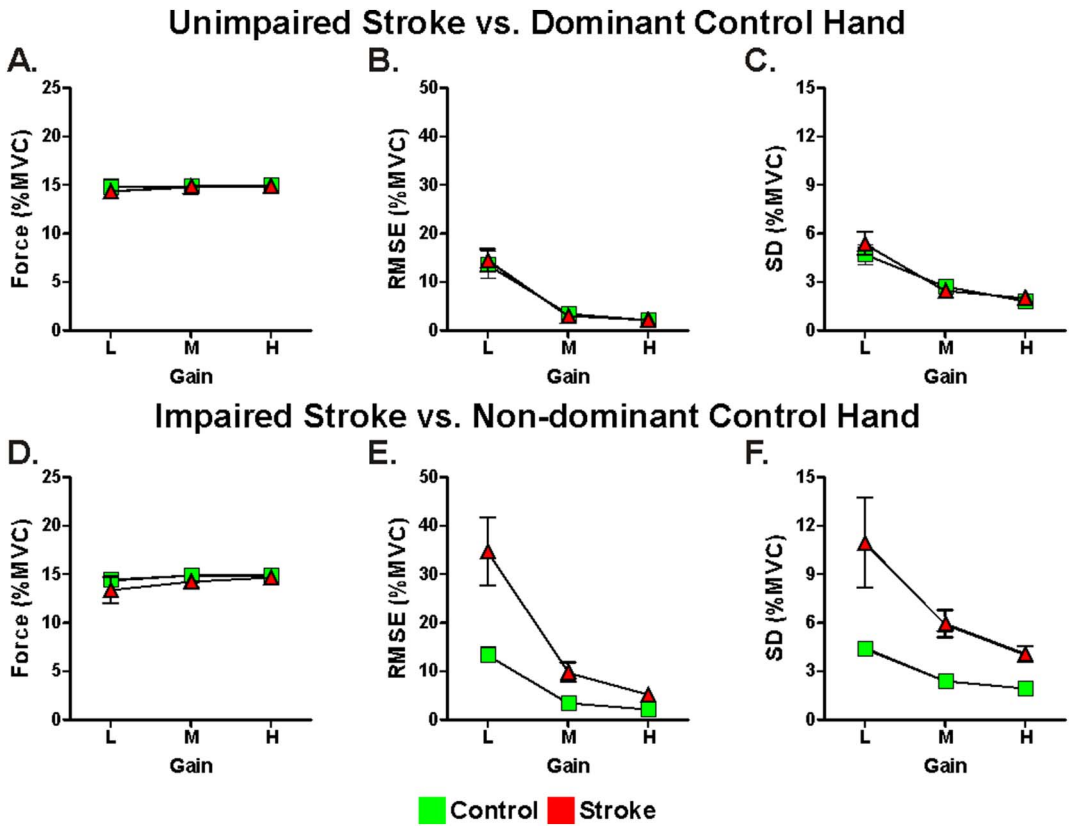

Fig. 3. Force measures.
Mean values for unimpaired/dominant hand force amplitude (A), force error (B), and force variability (C) are shown for control subjects (green) and stroke subjects (red) for all gain levels. Mean values for the impaired/non-dominant hand force amplitude (D), force error (E), and force variability is also shown. Each data point represents the group mean at each level of visual gain, and error bars represent ± SEM.

3.2.3. Force variability

Fig. 3C and F shows mean force variability for the stroke and control groups at each gain level for each hand. A two-way (group × gain) ANOVA on the unimpaired/dominant hand revealed a main effect of gain [$F(1.25, 34.93) = 57.39$; $P < 0.001$; $\eta^2 = 0.67$], showing a reduction in variability with an increase in visual gain (low > medium > high; all adjusted $P < 0.01$). There was no significant effect of group [$F(1, 28) = 0.15$; $P = 0.702$] and no group × gain interaction [$F(1.25, 34.93) = 1.09$; $P = 0.319$].

Fig. 3F shows data for the impaired/non-dominant hand. The corresponding two-way ANOVA on force variability revealed significant main effects of group [$F(1, 28) = 13.03$; $P = 0.001$; $\eta^2 = 0.32$] and gain [$F(1.12, 31.32) = 9.30$; $P = 0.004$; $\eta^2 = 0.25$], but no group × gain interaction [$F(1.12, 31.32) = 1.97$; $P = 0.17$]. Force variability was greater in the stroke group compared to the control group collapsed across the three gain levels. The main effect of gain was driven by a progressive decrease in force variability as visual gain was increased (low > medium > high; all adjusted P's < 0.05). Difference in force variability between the stroke and control groups was approximately 6%MVC at low visual gain, whereas the between group difference decreased at medium gain (~4%MVC) and high gain (~2%MVC).

3.3. Voxelwise analysis

3.3.1. Main effects of gain

Group-level statistical analysis of all three visual gain conditions revealed 28 clusters which showed significant gain-related differences in brain activity. Table 3 lists the location and composition of each cluster. Follow-up t-tests ($P < 0.05$, Bonferroni corrected) were performed to determine the specific gain levels which showed differences in activity. Fig. 4 shows the average BOLD percent signal change amplitude at each gain level collapsed across group. As shown in Fig. 4, functional activity across regions of the visuomotor network increased for both groups with an increase in gain level. Specifically, Fig. 4A shows that mean BOLD amplitude in contralateral V3/V5 increased from 0.28 at the low gain level to 0.59 at the medium gain level and 0.85 at the high gain level. Fig. 4C shows that BOLD amplitude in ipsilateral V3/V5 was 0.26 (low gain), 0.56 (medium gain), and 0.83 (high gain). Gain-related increases in BOLD amplitude were also found bilaterally in the inferior parietal lobule (IPL) in the contralateral hemisphere (Fig. 4D: low gain = 0.28, medium gain = 0.52, and high gain = 0.70) and the ipsilateral hemisphere (Fig. 4E: low gain = 0.18, medium gain = 0.53, and high gain = 0.64). Fig. 4B shows increases in BOLD amplitude in the medial wall of both hemispheres in supplementary motor area (SMA) (low gain = 0.28, medium gain = 0.53, and high gain = 0.61). Table 3 shows that an increase in gain led to similar progressive increases in the BOLD amplitude across many key regions of the visuomotor network including the cerebellar lobule VIIb, ventral premotor cortex (PMv), and caudate and putamen in the basal ganglia.

3.3.2. Main effect of group

A main effect of group was found in 15 clusters. Table 4 lists the location and composition of each cluster. Follow-up t-tests ($P < 0.05$, Bonferroni corrected) revealed that the stroke group had increased BOLD amplitude in 13/15 regions. In the contralateral hemisphere, the stroke group had increased activity in regions including the middle temporal gyrus, middle frontal gyrus, and superior temporal gyrus. In the ipsilateral hemisphere, the stroke group showed increased activity in clusters of voxels that were localized to M1/S1, inferior parietal lobule, PMv, and V3/V5. As shown in Table 4, the cluster size for regions which showed a group difference in BOLD amplitude (stroke >

Table 3
The regions demonstrating a gain effect identified by the voxelwise analysis.

	Peak *F*-statistic	CoM (MNI)			Volume (mm^3)	Gain effect (Bonferroni corrected *t*-tests)		
		x	y	z				
Gain effect						Low vs. medium	Low vs. high	Medium vs. high
Contralateral hemisphere								
V3/V5	21.3	43.9	−73.2	3.6	11,097	M > L	H > L	H > M
Inferior parietal lobule	16.4	33.8	−46.7	54.1	4239	–	H > L	–
Supramarginal gyrus	10.4	56.0	−37.0	28.1	1080	–	H > L	–
V3/V5	13.0	30.1	−72.4	33.1	702	–	H > L	–
*Lobule VIIb	13.0	10.4	−72.1	−43.3	675	M > L	H > L	–
Inferior temporal gyrus	13.0	53.9	−40.3	−18.9	270	–	H > L	–
Putamen	10.2	23.0	18.7	3.9	243	M > L	H > L	–
Inferior frontal gyrus	8.5	42.7	26.2	−1.3	243	–	H > L	H > M
Middle cingulum	9.4	11.5	−24.3	48.0	216	–	H > L	–
V3/V5	9.3	14.3	−93.0	20.3	216	M > L	H > L	–
Fusiform gyrus	11.4	32.2	−62.7	−8.6	216	L > M	L > H	–
Ipsilateral hemisphere								
SMA	17.5	−0.4	−5.4	61.9	11,502	M > L	H > L	–
V3/V5	25.2	−39.6	−78.2	2.7	9720	M > L	H > L	–
Inferior parietal lobule	19.7	−32.9	−50.3	54.5	4509	M > L	H > L	–
Putamen	15.8	−24.5	−11.8	15.3	2538	M > L	H > L	–
Thalamus	21.6	−19.5	−25.0	−0.8	1971	–	H > L	–
Insula	15.3	−32.7	14.0	9.1	1161	–	H > L	–
*Lobule VIIb	15.4	−17.9	−70.9	−46.6	864	M > L	H > L	–
PMv	14.9	−58.1	0.2	10.5	594	M > L	H > L	–
V3/V5	9.7	−27.7	−70.1	32.9	567	–	H > L	–
V3/V5	7.7	−46.7	−29.9	21.8	513	M > L	H > L	–
Fusiform gyrus	16.3	−33.3	−56.3	−20.1	486	M > L	H > L	–
PMv	15.9	−42.5	−1.3	10.9	459	–	H > L	–
Postcentral gyrus	10.0	−65.7	−20.4	13.7	405	M > L	H > L	–
PMv	11.7	−41.5	4.2	26.3	297	–	H > L	–
Caudate nucleus	8.2	−1.9	1.3	10.4	297	–	H > L	–
*Lobule VI	11.1	−18.1	−69.7	−21.0	243	M > L	H > L	–
Superior frontal gyrus	9.3	−22.0	−7.0	79.5	216	–	H > L	–

The anatomical regions of activation, peak *F*-statistic, MNI coordinates (CoM), and volume of each cluster are reported. SUIT derived clusters marked with *.

control) was the largest in M1/S1 on the ipsilateral hemisphere: the ipsilateral M1/S1 cluster had a volume 4.75 times larger than next largest cluster. Mean BOLD amplitude was 0.74 for the stroke group and 0.12 for the control group (Fig. 5). Note that the ipsilateral hemisphere corresponds with the contralesional hemisphere in the stroke group and non-dominant hemisphere in controls. To determine whether our findings were specific to the non-dominant hand in controls, we conducted a secondary ROI analysis. We extracted the BOLD signal from the ipsilateral M1/S1 while controls performed the force task with their dominant hand. We found that the stroke group still showed significantly higher BOLD signal compared to control subjects in ipsilateral M1/S1 (see Supplemental Material).

3.3.3. Gain × group interactions

Group-level statistical analysis identified 12 clusters whose activity showed an interaction effect between gain and group. Table 5 lists the location and composition of each cluster. Follow-up *t*-tests ($P < 0.05$, Bonferroni corrected) were conducted between groups at each level of visual gain. Fig. 6 shows a 3D brain image with yellow clusters identifying regions that showed a significant interaction effect, orange clusters identifying regions that showed a significant gain effect, and blue clusters identifying regions that showed a significant group effect. Interaction effects were localized to IPL, supramarginal gyrus, and V3/V5 in the contralateral hemisphere, and regions including V3/V5, and cerebellar lobules VI and VIIb in the ipsilateral hemisphere. As shown in Fig. 6A and B, BOLD amplitude in supramarginal gyrus and IPL in the contralateral hemisphere were comparable between the stroke group (red squares) and control group (green squares) across the low and medium gain levels, but at the high gain the stroke group (supramarginal gyrus = 1.29; IPL = 0.84) exhibited greater BOLD amplitude than controls (supramarginal gyrus = 0.47; IPL = 0.44). These regions were adjacent to the areas where significant main effects of gain were found as shown by their close proximity to orange clusters. The BOLD amplitude in cerebellar lobules VI (Fig. 6C) and VIIb (Fig. 6D) in the ipsilateral hemisphere was significantly increased in the stroke group at the medium and high levels of gain as compared to controls. These changes in the cerebellar lobules VI and VIIb were spatially distinct from clusters that varied as a function of gain or group.

4. Discussion

Here, we combined a visually guided grip force task with functional MRI to understand how changes in the gain of visual feedback alter brain activity in the chronic phase after stroke. Brain imaging analyses focused on brain activation when force was produced by the most impaired hand of the stroke group as compared to the non-dominant hand of the control group. Our experiment produced three novel results. First, gain-related improvements in force control in both the stroke and control group were associated with an increase in activity in the visuomotor network, including V3/V5, IPL, PMv, and SMA. Second, the stroke group showed gain-related increases in activity in additional regions of lobules VI and VIIb of the ipsilateral cerebellum. Third, relative to the control group, the stroke group showed increased activity in the ipsilateral M1, and activity in this region did not vary as a function of gain level. The visuomotor network, cerebellum, and ipsilateral M1 have each been targeted in rehabilitation interventions after stroke, and our findings provide new insight into the role these regions play during a precisely-controlled motor task in the chronic phase after stroke.

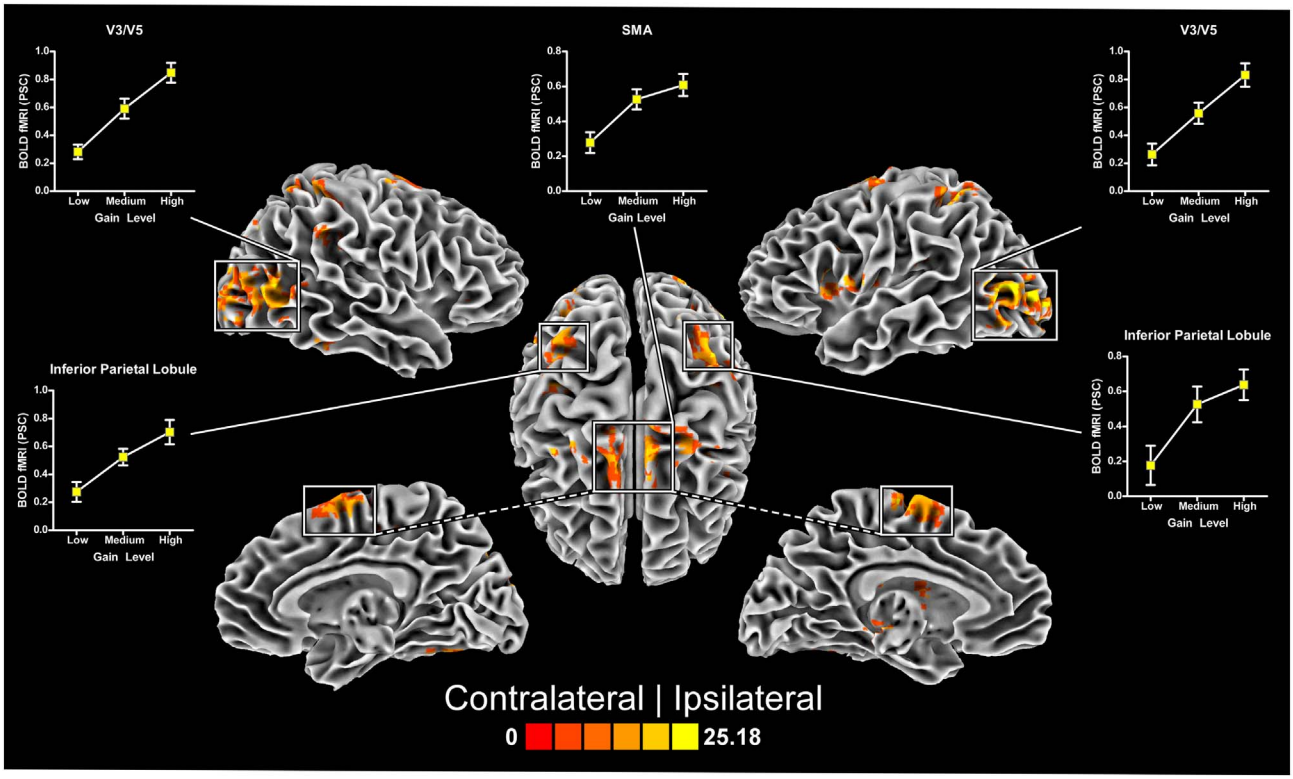

Fig. 4. Main effect of gain.
Results of the main effect of gain obtained from the 3dANOVA in AFNI. Statistical maps were thresholded at $P = 0.005$ and cluster extent of 216 mm^3 for the cortex and 162 mm^3 for the cerebellum. The statistic displayed is the *F*-statistic, with brighter colors indicating more significant voxels which demonstrated changes in BOLD signal with a change in visual gain. Regions with visuomotor importance are marked, with the plots connected to them displaying the average BOLD amplitude at each gain level (yellow data points). Error bars indicate ± SEM, between gain differences are shown in Table 3 ($P < 0.05$, Bonferroni corrected).

4.1. Visuomotor network

Across both groups, increases in visual gain lead to reductions in force error, reductions in force variability, and increases in functional activity in the visuomotor network in regions including V3/V5, bilateral IPL, ipsilateral PMv, bilateral SMA, and cerebellar lobules VI and VIIb. Implementing a precisely controlled visuomotor task to elicit activity in this broadly distributed visuomotor system corroborates previous electrophysiology and imaging evidence which links visuomotor processing with activity in this network (Ebner and Fu, 1997; Hoshi and Tanji, 2006; Krakauer et al., 2004; Roitman et al., 2009; Vaillancourt et al., 2006; Vaillancourt et al., 2003; van Eimeren et al., 2006). It is well established that viewing motion stimuli leads to increases in neural activity in regions of the extrastriate visual cortex

Table 4
The regions demonstrating a group effect identified by the voxelwise analysis.

	Peak *F*-statistic	CoM (MNI)			Volume (mm^3)	Group effect (Bonferroni corrected *t*-tests)
		x	y	z		
Group effect						Stroke vs. control
Contralateral hemisphere						
Middle temporal gyrus	17.6	47.7	− 40.2	− 11.9	486	C < S
Middle frontal gyrus	16.6	30.7	55.8	38.3	459	C < S
Angular gyrus	16.3	51.2	− 62.0	24.6	297	C < S
*Lobule VIIb	10.5	20.0	− 76.0	− 50.0	270	C > S
Superior temporal gyrus	14.0	43.8	− 18.7	1.6	216	C < S
Ipsilateral hemisphere						
M1/S1	40.8	− 46.1	− 17.8	44.4	3726	C < S
Inferior parietal lobule	21.8	− 55.4	− 32.2	36.8	783	C < S
Postcentral gyrus	19.5	− 57.6	− 16.4	19.6	459	C > S
S1	23.5	− 40.0	− 33.3	69.3	459	C < S
PMv	19.2	− 45.3	7.6	33.7	405	C < S
Insula	16.6	− 39.8	1.5	− 3.6	324	C < S
V3/V5	16.9	− 38.6	− 78.5	2.8	324	C < S
Superior temporal gyrus	19.1	− 49.5	− 18.4	4.7	324	C < S
Hippocampus	12.6	− 18.2	− 27.0	− 8.3	243	C < S
V3/V5	13.8	− 27.3	− 63.1	39.0	243	C < S

The anatomical regions of activation, peak *F*-statistic, MNI coordinates (CoM), and volume of each cluster are reported. SUIT derived clusters marked with *.

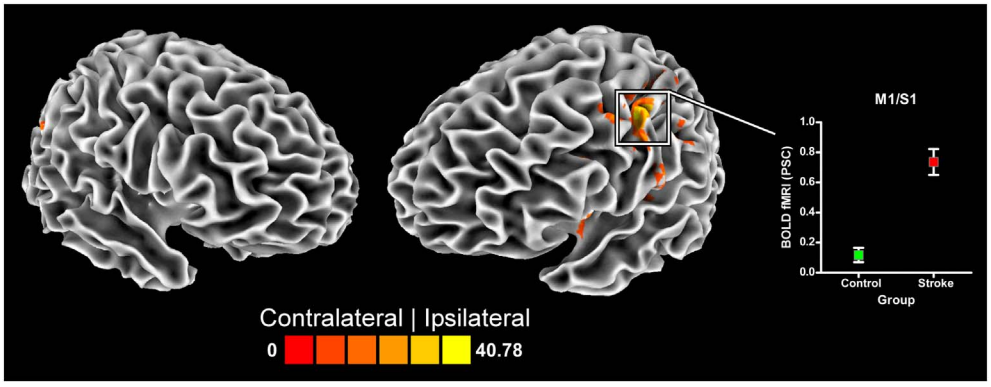

Fig. 5. Main effect of group.
Results of the main effect of group obtained from the 3dANOVA in AFNI. Statistical maps were thresholded at $P = 0.005$ and extent of 216 mm^3 for the cortex and 162 mm^3 for the cerebellum. The statistic display is the *F*-statistic, with brighter colors indicating more significant voxels which demonstrated a difference in BOLD signal between groups averaged across gain levels. The average BOLD amplitude for the control group (green) and stroke group (red) is shown. The stroke group displayed increased BOLD amplitude change, compared to controls, at all gain levels ($P < 0.05$, Bonferroni corrected). Error bars indicate ± SEM. Between group differences across all gain levels are shown in Table 4.

including areas V3/V5 (Martinez-Trujillo et al., 2007; Paradis et al., 2000; Sack et al., 2006), and that visual motion stimuli affect neural signals in the motor cortex via projections from the parietal cortex to the premotor cortex (Caminiti et al., 1996; Wise et al., 1997). Parietal cortex activation during visuomotor processing has been interpreted as reflecting visuospatial processing (Krakauer et al., 2004), visuomotor error correction (Grefkes et al., 2004), and coupled with the increase in activity in PMv, provides evidence that function of the fronto-parietal circuit is at least partially preserved after stroke. There is now extensive evidence to support the position that the fronto-parietal circuit plays a major role in visually-guided precision motor control (Davare et al., 2006; Ehrsson et al., 2000), and disruption of either of these regions leads to deficits in online visuomotor corrections (Della-Maggiore et al., 2004; Desmurget et al., 1999; Lee and van Donkelaar, 2006; Van Donkelaar et al., 2000). The amplitude of activation in the visuomotor system was not markedly different between groups which suggest that the increase in force error and force variability could not be attributed to deficits in functional activity within this network. Hence, our observations extend previous evidence in healthy younger adults by showing that increases in visual gain engage the extrastriate visual cortex and the fronto-parietal visuomotor network in older adults and in individuals in the chronic phase after stroke (Coombes et al., 2010).

Importantly, when the level of visual gain increased, the stroke group exhibited elevated functional activity in the contralateral V3/V5 and IPL while reducing force error with the impaired hand. These novel findings support a proposition that increasing visual feedback gain is a viable option for engaging larger regions of the visuomotor network in order to improve force control after stroke (Bonan et al., 2004b; Tunik et al., 2013). Indeed, although force error and force variability remained higher in the stroke group across all gain levels, as the between group difference in behavior was attenuated with an increase in visual gain, the stroke group showed an increase in the number of active clusters within the visuomotor network. Gain-related increases in activity were also evident across both groups in lobules VI and VIIb in the ipsilateral cerebellum. The stroke group also showed activity within these same lobules that was spatially distinct from those that varied as a function of gain. Evidence from studies in animals (Kitazawa et al., 1998; Liu et al., 2003) and humans (Spraker et al., 2012; Vaillancourt et al., 2006) have demonstrated that the posterior cerebellum is a crucial region that contributes to visually-guided error correction. Indeed, the cerebellum may transfer visual information into corrective signals to alter ongoing motor output to minimize motor variability (Stein and Glickstein, 1992; Vaillancourt et al., 2006). However, previous findings in younger healthy adults did not find gain-related increases in cerebellar activity, with the cerebellum being equally active across all levels of visual gain (Coombes et al., 2010). In the context of these previous findings, one interpretation is that during visuomotor processing, age may lead to an increase in the engagement of the cerebellum to support the error correction process, and that the engagement of these cerebellar regions is augmented after stroke. Such a position is consistent with other observations which demonstrate a central role for the cerebellum in motor adaptation (Bastian, 2006, 2008; Rabe et al., 2009; Thach et al., 1992), and recent stimulation paradigms that target cerebellar activity to influence motor function in rodent models

Table 5
The regions demonstrating a group x gain interaction identified by the voxelwise analysis.

	Peak *F*-statistic	CoM (MNI)			Volume (mm^3)	Group effect (Bonferroni corrected *t*-tests)		
		x	y	z		Low	Medium	High
Group × gain interaction						Stroke vs. control		
Contralateral hemisphere								
Inferior parietal lobule	12.2	32.0	−54.8	55.4	432	–	–	–
Supramarginal gyrus	9.9	56.8	−40.2	31.4	378	–	–	–
V3/V5	14.6	28.6	−87.5	14.5	270	–	–	S > C
Ipsilateral hemisphere								
Thalamus	17.5	−25.1	−25.5	−1.5	675	–	–	S > C
Insula	12.4	−34.4	12.5	9.6	675	–	–	S > C
V3/V5	10.1	−29.4	−81.1	9.4	270	–	–	S > C
Calcarine	7.6	−7.3	−78.4	9.9	270	–	–	S > C
*Lobule VI	8.3	−30.2	−62.4	−25.2	270	–	–	S > C
Middle temporal gyrus	10.9	−58.7	−61.6	10.6	243	–	–	S > C
Thalamus	12.7	−3.3	−25.6	−6.9	216	C > S	S > C	–
Superior temporal gyrus	12.6	−38.7	−8.5	−7.0	216	–	–	S > C
*Lobule VIIb	9.7	−23.3	−70.9	−49.4	162	–	S > C	–

The anatomical regions of activation, peak *F*-statistic, MNI coordinates (CoM), and volume of each cluster are reported. SUIT derived clusters marked with *.

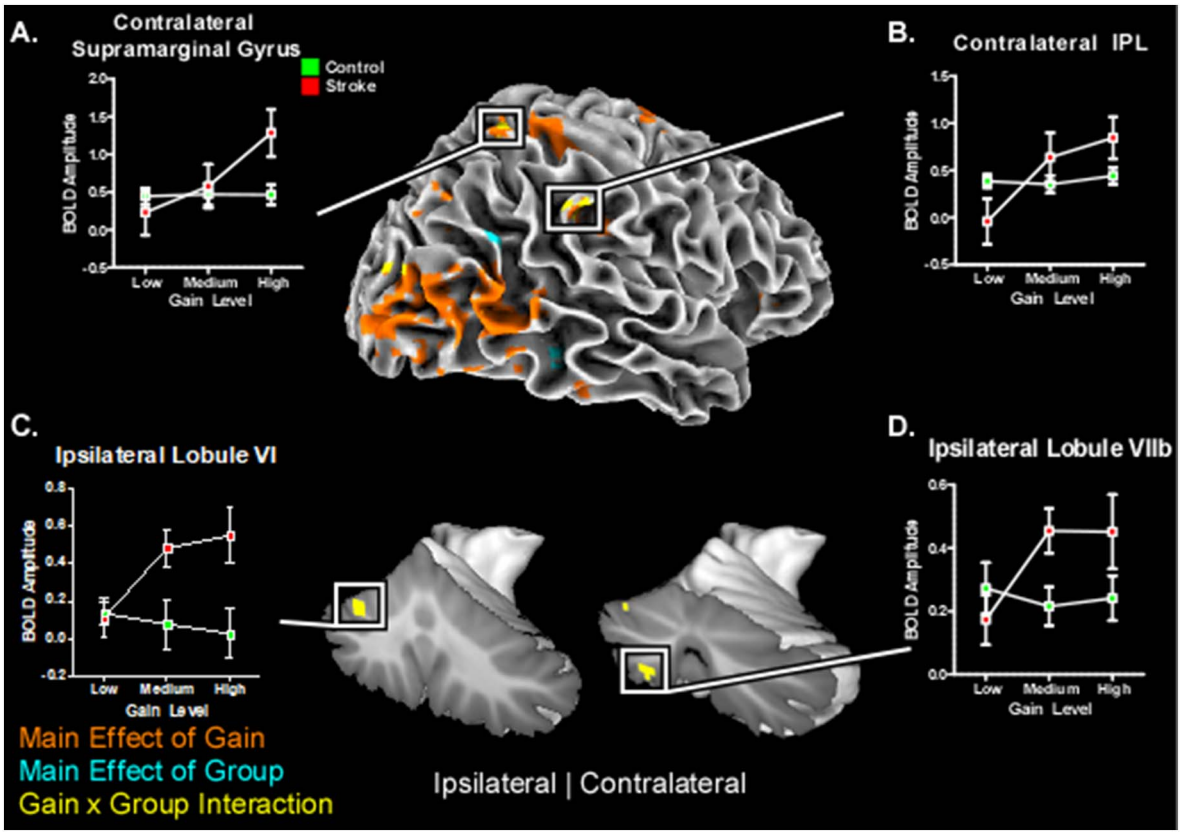

Fig. 6. Gain × group interaction.
A conjunction showing the main effect of gain (orange), main effect of group (blue), and group × gain interaction (yellow) is shown. Results of the group x gain interaction were obtained from 3dANOVA in AFNI. Statistical maps were thresholded at $P = 0.005$ and extent of 216 mm^3 for the cortex and 162 mm^3 for the cerebellum. Group x gain interaction regions with visuomotor importance are marked, with the plots connected to them displaying the average BOLD amplitude at each gain level for both groups (control: green, stroke: red). Error bars indicate ± SEM. Between-group differences at each gain level are shown in Table 5 ($P < 0.05$, Bonferroni corrected).

(Park et al., 2015), as well as humans (Ferrucci and Priori, 2014; Jalali et al., 2017; Jayaram et al., 2011; Samaei et al., 2017).

4.2. Ipsilateral primary motor cortex

The stroke group showed increased activity in the ipsilateral primary motor cortex during force production by the impaired hand across all levels of visual gain. Our finding is consistent with other evidence from studies in humans and animals which identify increased activity in ipsilateral M1 after stroke (Biernaskie et al., 2005; Buetefisch, 2015; Touvykine et al., 2016). Here, we show that whereas force error, force variability, and activation of the visuomotor network are influenced by a change in visual gain, activity in ipsilateral primary motor cortex was not. Hence, task-related activity in ipsilateral M1 differentiated the stroke group from the control group, but ipsilateral M1 activity was not sensitive to changes in the characteristics of the visuomotor task.

Since the first report of bilateral activity in stroke patients moving their most impaired hand (Chollet et al., 1991), a role for ipsilateral M1 in cortical reorganization after stroke has been repeatedly demonstrated using a range of neurophysiological assays including PET, fMRI, EEG, and TMS (Auriat et al., 2015; Calautti and Baron, 2003; Rehme et al., 2012; Serrien et al., 2004). However, consensus has yet to be reached on the exact role of ipsilateral M1 during movements of the impaired hand after stroke, though it is generally considered to be maladaptive to recovery (Buetefisch, 2015). Bilateral M1 BOLD activity has been shown to increase with increased force output (Cramer et al., 2002; Perez and Cohen, 2009), and BOLD activity in ipsilateral M1 has previously been demonstrated in healthy adults during complex motor tasks and tasks that demand greater precision (Buetefisch et al., 2014; Hummel et al., 2003; Verstynen et al., 2005). These findings have led to the interpretation that stroke-related increases in ipsilateral M1 activity may reflect an increase in task difficulty or effort. However, evidence from a well-controlled longitudinal study that manipulated target force based on a relative level (i.e., % of MVC), or an absolute level (kg) of force production suggests that over activation of ipsilateral activity in M1 early after stroke may better reflect reorganization in the motor system rather than an increase in effort (Bonstrup et al., 2015). These data highlight the importance of using precisely controlled feedback based performance tasks when comparing brain activity between stroke and control groups. Other evidence shows that interfering with activity in ipsilateral M1 using short bursts of TMS facilitate finger tapping frequency in the sub-acute phase after stroke, but has no impact 3 months after stroke (Volz et al., 2017). These data suggest that the role of ipsilateral M1 during movements of the impaired hand is tightly coupled to time since stroke. Taken together, these findings suggest that while ipsilateral M1 activity scales with force requirement, there is little direct evidence to support the position that ipsilateral M1 activity scales with an increase in task difficulty or effort in the chronic phase after stroke.

Increased activity in ipsilateral M1 has been shown during both synergistic (less skilled) and non-synergistic (more skilled) hand movements, with differences in task difficulty reflected in the engagement of an extended ipsilateral motor network rather than in an increase in ipsilateral M1 activity (Schaechter and Perdue, 2008). Bilateral activity in primary and secondary motor areas has also been observed in chronic stroke during unimanual finger movements, even when controlling for the possibility of mirror movements (Butefisch et al., 2005; Calautti and Baron, 2003; Ward et al., 2003a, 2003b). We found no evidence of mirror movements in the current study as indexed by the absence of force production by the passive unimpaired/

dominant hand. Ipsilateral cortical activity in the primary motor cortex is also observed in unilateral upper extremity amputees when moving their intact hand (Bogdanov et al., 2012; Philip and Frey, 2014), but whether this ipsilateral activity is functionally relevant remains an open question. The current findings are the first to show that parametrically scaling the properties of visual feedback do not lead to scaling of brain activity in ipsilateral M1 in the chronic phase after stroke, even though robust changes in task performance and activity in other regions of the visuomotor network were evident.

Repetitive TMS and effective connectivity studies in humans suggest that ipsilateral M1 inhibits contralateral M1 during impaired hand function (Grefkes et al., 2010; Murase et al., 2004; Nowak et al., 2008; Takeuchi et al., 2005). Other evidence, however, shows that the non-lesioned hemisphere does not exert a functional inhibitory effect on paretic limb motor output when measured during task performance (Dimyan et al., 2014), and may even support ipsilateral M1 function (Lotze et al., 2006; Rehme et al., 2011). Nevertheless, increased activity in ipsilateral M1 during less use or poorer function of the paretic arm (Cramer et al., 2007; Kokotilo et al., 2009; Kokotilo et al., 2010), and increased interhemispheric inhibition has motivated neuromodulatory practices such as inhibitory rTMS and cathodal tDCS to the ipsilateral hemisphere. Results have also been mixed (Rose et al., 2014), and recent meta-analyses have found inconclusive results regarding the efficacy of inhibitory rTMS on functional outcomes (Graef et al., 2016; Smith and Stinear, 2016). Moreover, the influence of factors such as time after stroke, impairment level, age, and lesion load on cortical activity have been extensively studied, but a meta-analysis showed no consistent association between ipsilateral M1 activation and time or impairment after stroke (Rehme et al., 2012). This position is consistent with data from a prospective cohort study that found that while there was indeed asymmetry of interhemispheric inhibition in the acute/subacute period, it remained asymmetrical over time and did not correspond to or predict recovery (Stinear et al., 2015; Volz et al., 2017) In the current study, it is not clear if increased activity helped or hindered force output in the stroke group and so it is not clear if the higher activity in ipsilateral M1 in the stroke group is functionally relevant or an epiphenomenon.

In conclusion, this study revealed that manipulating visual feedback in the chronic phase after stroke is a viable and useful option for reducing force error and force variability during grip force. Our observations also show that increasing visual gain leads to patterns of visuomotor network recruitment similar to age matched healthy controls. Furthermore, increases in gain led the stroke group to engage a greater number of regions within the visuomotor network to a greater extent than controls. The current study also provides new evidence on the role of ipsilateral M1 after stroke, because although activity in ipsilateral M1 was greater in stroke as compared to control subjects, it did not change with visual input or force output. Future studies that stimulate or inhibit ipsilateral M1 function during a visual gain task performed by the impaired hand would address whether ipsilateral M1 activity is functionally relevant.

Funding

This work was supported by the American Heart Association (15GRNT25700431) and the James and Esther King Biomedical Research Program, Florida Department of Health (3KN01).

Acknowledgements

MRI data collection was supported through the National High Magnetic Field Laboratory and obtained at the Advanced Magnetic Resonance Imaging and Spectroscopy facility in the McKnight Brain Institute of the University of Florida.

Conflict of interest

Stephen A. Coombes is co-founder and manager of Neuroimaging Solutions, LLC.

Appendix A. Supplementary data

Supplementary data to this article can be found online at https://doi.org/10.1016/j.nicl.2017.11.012.

References

Archer, D.B., Misra, G., Patten, C., Coombes, S.A., 2016. Microstructural properties of premotor pathways predict visuomotor performance in chronic stroke. Hum. Brain Mapp. 37, 2039–2054.
Archer, D.B., Vaillancourt, D.E., Coombes, S.A., 2017. A template and probabilistic atlas of the human sensorimotor tracts using diffusion MRI. Cereb. Cortex 1–15.
Auriat, A.M., Neva, J.L., Peters, S., Ferris, J.K., Boyd, L.A., 2015. A review of transcranial magnetic stimulation and multimodal neuroimaging to characterize post-stroke neuroplasticity. Front. Neurol. 6, 226.
Bagce, H.F., Saleh, S., Adamovich, S.V., Tunik, E., 2012. Visuomotor gain distortion alters online motor performance and enhances primary motor cortex excitability in patients with stroke. Neuromodulation 15, 361–366.
Bastian, A.J., 2006. Learning to predict the future: the cerebellum adapts feedforward movement control. Curr. Opin. Neurobiol. 16, 645–649.
Bastian, A.J., 2008. Understanding sensorimotor adaptation and learning for rehabilitation. Curr. Opin. Neurol. 21, 628–633.
Bestmann, S., Swayne, O., Blankenburg, F., Ruff, C.C., Teo, J., Weiskopf, N., Driver, J., Rothwell, J.C., Ward, N.S., 2010. The role of contralesional dorsal premotor cortex after stroke as studied with concurrent TMS-fMRI. J. Neurosci. 30, 11926–11937.
Biernaskie, J., Szymanska, A., Windle, V., Corbett, D., 2005. Bi-hemispheric contribution to functional motor recovery of the affected forelimb following focal ischemic brain injury in rats. Eur. J. Neurosci. 21, 989–999.
Bogdanov, S., Smith, J., Frey, S.H., 2012. Former hand territory activity increases after amputation during intact hand movements, but is unaffected by illusory visual feedback. Neurorehabil. Neural Repair 26, 604–615.
Bohannon, R.W., Smith, M.B., 1987. Interrater reliability of a modified Ashworth scale of muscle spasticity. Phys. Ther. 67, 206–207.
Bonan, I.V., Colle, F.M., Guichard, J.P., Vicaut, E., Eisenfisz, M., Tran Ba Huy, P., Yelnik, A.P., 2004a. Reliance on visual information after stroke. Part I: balance on dynamic posturography. Arch. Phys. Med. Rehabil. 85, 268–273.
Bonan, I.V., Yelnik, A.P., Colle, F.M., Michaud, C., Normand, E., Panigot, B., Roth, P., Guichard, J.P., Vicaut, E., 2004b. Reliance on visual information after stroke. Part II: effectiveness of a balance rehabilitation program with visual cue deprivation after stroke: a randomized controlled trial. Arch. Phys. Med. Rehabil. 85, 274–278.
Bonstrup, M., Schulz, R., Cheng, B., Feldheim, J., Zimerman, M., Thomalla, G., Hummel, F.C., Gerloff, C., 2015. Evolution of brain activation after stroke in a constant-effort versus constant-output motor task. Restor. Neurol. Neurosci. 33, 845–864.
Brewer, B.R., Fagan, M., Klatzky, R.L., Matsuoka, Y., 2005. Perceptual limits for a robotic rehabilitation environment using visual feedback distortion. IEEE Trans. Neural. Syst. Rehabil. Eng. 13, 1–11.
Brewer, B.R., Klatzky, R., Matsuoka, Y., 2008. Visual feedback distortion in a robotic environment for hand rehabilitation. Brain Res. Bull. 75, 804–813.
Buetefisch, C.M., 2015. Role of the contralesional hemisphere in post-stroke recovery of upper extremity motor function. Front. Neurol. 6, 214.
Buetefisch, C.M., Revill, K.P., Shuster, L., Hines, B., Parsons, M., 2014. Motor demand-dependent activation of ipsilateral motor cortex. J. Neurophysiol. 112, 999–1009.
Butefisch, C.M., Kleiser, R., Korber, B., Muller, K., Wittsack, H.J., Homberg, V., Seitz, R.J., 2005. Recruitment of contralesional motor cortex in stroke patients with recovery of hand function. Neurology 64, 1067–1069.
Calautti, C., Baron, J.C., 2003. Functional neuroimaging studies of motor recovery after stroke in adults: a review. Stroke 34, 1553–1566.
Caminiti, R., Ferraina, S., Johnson, P.B., 1996. The sources of visual information to the primate frontal lobe: a novel role for the superior parietal lobule. Cereb. Cortex 6, 319–328.
Carter, A.R., Connor, L.T., Dromerick, A.W., 2010. Rehabilitation after stroke: current state of the science. Curr. Neurol. Neurosci. Rep. 10, 158–166.
Chang, S.H., Francisco, G.E., Zhou, P., Rymer, W.Z., Li, S., 2013. Spasticity, weakness, force variability, and sustained spontaneous motor unit discharges of resting spastic-paretic biceps brachii muscles in chronic stroke. Muscle Nerve 48, 85–92.
Chollet, F., DiPiero, V., Wise, R.J., Brooks, D.J., Dolan, R.J., Frackowiak, R.S., 1991. The functional anatomy of motor recovery after stroke in humans: a study with positron emission tomography. Ann. Neurol. 29, 63–71.
Coombes, S.A., Corcos, D.M., Sprute, L., Vaillancourt, D.E., 2010. Selective regions of the visuomotor system are related to gain-induced changes in force error. J. Neurophysiol. 103, 2114–2123.
Cramer, S.C., Nelles, G., Benson, R.R., Kaplan, J.D., Parker, R.A., Kwong, K.K., Kennedy, D.N., Finklestein, S.P., Rosen, B.R., 1997. A functional MRI study of subjects recovered from hemiparetic stroke. Stroke 28, 2518–2527.
Cramer, S.C., Weisskoff, R.M., Schaechter, J.D., Nelles, G., Foley, M., Finklestein, S.P., Rosen, B.R., 2002. Motor cortex activation is related to force of squeezing. Hum. Brain Mapp. 16, 197–205.

Cramer, S.C., Parrish, T.B., Levy, R.M., Stebbins, G.T., Ruland, S.D., Lowry, D.W., Trouard, T.P., Squire, S.W., Weinand, M.E., Savage, C.R., Wilkinson, S.B., Juranek, J., Leu, S.Y., Himes, D.M., 2007. Predicting functional gains in a stroke trial. Stroke 38, 2108–2114.
Davare, M., Andres, M., Cosnard, G., Thonnard, J.L., Olivier, E., 2006. Dissociating the role of ventral and dorsal premotor cortex in precision grasping. J. Neurosci. 26, 2260–2268.
Della-Maggiore, V., Malfait, N., Ostry, D.J., Paus, T., 2004. Stimulation of the posterior parietal cortex interferes with arm trajectory adjustments during the learning of new dynamics. J. Neurosci. 24, 9971–9976.
Desikan, R.S., Segonne, F., Fischl, B., Quinn, B.T., Dickerson, B.C., Blacker, D., Buckner, R.L., Dale, A.M., Maguire, R.P., Hyman, B.T., Albert, M.S., Killiany, R.J., 2006. An automated labeling system for subdividing the human cerebral cortex on MRI scans into gyral based regions of interest. NeuroImage 31, 968–980.
Desmurget, M., Epstein, C.M., Turner, R.S., Prablanc, C., Alexander, G.E., Grafton, S.T., 1999. Role of the posterior parietal cortex in updating reaching movements to a visual target. Nat. Neurosci. 2, 563–567.
Diedrichsen, J., 2006. A spatially unbiased atlas template of the human cerebellum. NeuroImage 33, 127–138.
Diedrichsen, J., Balsters, J.H., Flavell, J., Cussans, E., Ramnani, N., 2009. A probabilistic MR atlas of the human cerebellum. NeuroImage 46, 39–46.
Dimyan, M.A., Perez, M.A., Auh, S., Tarula, E., Wilson, M., Cohen, L.G., 2014. Non-paretic arm force does not over-inhibit the paretic arm in chronic post-stroke hemiparesis. Arch. Phys. Med. Rehabil. 95 (5), 849–856.
Ebner, T.J., Fu, Q., 1997. What features of visually guided arm movements are encoded in the simple spike discharge of cerebellar Purkinje cells? Prog. Brain Res. 114, 431–447.
Ehrsson, H.H., Fagergren, A., Jonsson, T., Westling, G., Johansson, R.S., Forssberg, H., 2000. Cortical activity in precision- versus power-grip tasks: an fMRI study. J. Neurophysiol. 83, 528–536.
Favre, I., Zeffiro, T.A., Detante, O., Krainik, A., Hommel, M., Jaillard, A., 2014. Upper limb recovery after stroke is associated with ipsilesional primary motor cortical activity: a meta-analysis. Stroke 45, 1077–1083.
Ferrucci, R., Priori, A., 2014. Transcranial cerebellar direct current stimulation (tcDCS): motor control, cognition, learning and emotions. NeuroImage 85 (Pt 3), 918–923.
Folstein, M.F., Folstein, S.E., McHugh, P.R., 1975. "Mini-mental state". A practical method for grading the cognitive state of patients for the clinician. J. Psychiatr. Res. 12, 189–198.
Fugl-Meyer, A.R., Jaasko, L., Leyman, I., Olsson, S., Steglind, S., 1975. The post-stroke hemiplegic patient. 1. A method for evaluation of physical performance. Scand. J. Rehabil. Med. 7, 13–31.
Gladstone, D.J., Danells, C.J., Black, S.E., 2002. The fugl-meyer assessment of motor recovery after stroke: a critical review of its measurement properties. Neurorehabil. Neural Repair 16, 232–240.
Graef, P., Dadalt, M.L., Rodrigues, D.A., Stein, C., Pagnussat Ade, S., 2016. Transcranial magnetic stimulation combined with upper-limb training for improving function after stroke: a systematic review and meta-analysis. J. Neurol. Sci. 369, 149–158.
Grafton, S.T., Mazziotta, J.C., Woods, R.P., Phelps, M.E., 1992. Human functional anatomy of visually guided finger movements. Brain J. Neurol. 115 (Pt 2), 565–587.
Grefkes, C., Ritzl, A., Zilles, K., Fink, G.R., 2004. Human medial intraparietal cortex subserves visuomotor coordinate transformation. NeuroImage 23, 1494–1506.
Grefkes, C., Nowak, D.A., Wang, L.E., Dafotakis, M., Eickhoff, S.B., Fink, G.R., 2010. Modulating cortical connectivity in stroke patients by rTMS assessed with fMRI and dynamic causal modeling. NeuroImage 50, 233–242.
Haas, B.M., Bergstrom, E., Jamous, A., Bennie, A., 1996. The inter-rater reliability of the original and of the modified Ashworth scale for the assessment of spasticity in patients with spinal cord injury. Spinal Cord 34, 560–564.
Hoshi, E., Tanji, J., 2006. Differential involvement of neurons in the dorsal and ventral premotor cortex during processing of visual signals for action planning. J. Neurophysiol. 95, 3596–3616.
Hummel, F., Kirsammer, R., Gerloff, C., 2003. Ipsilateral cortical activation during finger sequences of increasing complexity: representation of movement difficulty or memory load? Clin. Neurophysiol. 114, 605–613.
Jalali, R., Miall, R.C., Galea, J.M., 2017. No consistent effect of cerebellar transcranial direct current stimulation (tDCS) on visuomotor adaptation. J. Neurophysiol. 00896, 02016.
Jayaram, G., Galea, J.M., Bastian, A.J., Celnik, P., 2011. Human locomotor adaptive learning is proportional to depression of cerebellar excitability. Cereb. Cortex 21, 1901–1909.
Kang, N., Cauraugh, J.H., 2015a. Bimanual force variability in chronic stroke: with and without visual information. Neurosci. Lett. 587, 41–45.
Kang, N., Cauraugh, J.H., 2015b. Force control in chronic stroke. Neurosci. Biobehav. Rev. 52, 38–48.
Kitazawa, S., Kimura, T., Yin, P.B., 1998. Cerebellar complex spikes encode both destinations and errors in arm movements. Nature 392, 494–497.
Kokotilo, K.J., Eng, J.J., Boyd, L.A., 2009. Reorganization of brain function during force production after stroke: a systematic review of the literature. J. Neurol. Phys. Ther. 33, 45–54.
Kokotilo, K.J., Eng, J.J., McKeown, M.J., Boyd, L.A., 2010. Greater activation of secondary motor areas is related to less arm use after stroke. Neurorehabil. Neural Repair 24, 78–87.
Krakauer, J.W., Ghilardi, M.F., Mentis, M., Barnes, A., Veytsman, M., Eidelberg, D., Ghez, C., 2004. Differential cortical and subcortical activations in learning rotations and gains for reaching: a PET study. J. Neurophysiol. 91, 924–933.
Lee, J.H., van Donkelaar, P., 2006. The human dorsal premotor cortex generates on-line error corrections during sensorimotor adaptation. J. Neurosci. 26, 3330–3334.
Li, S., Durand-Sanchez, A., Latash, M.L., 2014. Inter-limb force coupling is resistant to distorted visual feedback in chronic hemiparetic stroke. J. Rehabil. Med. 46, 206–211.
Lindberg, P.G., Roche, N., Robertson, J., Roby-Brami, A., Bussel, B., Maier, M.A., 2012. Affected and unaffected quantitative aspects of grip force control in hemiparetic patients after stroke. Brain Res. 1452, 96–107.
Liu, X.G., Robertson, E., Miall, R.C., 2003. Neuronal activity related to the visual representation of arm movements in the lateral cerebellar cortex. J. Neurophysiol. 89, 1223–1237.
Lodha, N., Naik, S.K., Coombes, S.A., Cauraugh, J.H., 2010. Force control and degree of motor impairments in chronic stroke. Clin. Neurophysiol. 121, 1952–1961.
Lodha, N., Coombes, S.A., Cauraugh, J.H., 2012a. Bimanual isometric force control: asymmetry and coordination evidence poststroke. Clin. Neurophysiol. 123, 787–795.
Lodha, N., Patten, C., Coombes, S.A., Cauraugh, J.H., 2012b. Bimanual force control strategies in chronic stroke: finger extension versus power grip. Neuropsychologia 50, 2536–2545.
Lotze, M., Markert, J., Sauseng, P., Hoppe, J., Plewnia, C., Gerloff, C., 2006. The role of multiple contralesional motor areas for complex hand movements after internal capsular lesion. J. Neurosci. Off. J. Soc. Neurosci. 26, 6096–6102.
Loubinoux, I., Dechaumont-Palacin, S., Castel-Lacanal, E., De Boissezon, X., Marque, P., Pariente, J., Albucher, J.F., Berry, I., Chollet, F., 2007. Prognostic value of FMRI in recovery of hand function in subcortical stroke patients. Cereb. Cortex 17, 2980–2987.
Marshall, R.S., Zarahn, E., Alon, L., Minzer, B., Lazar, R.M., Krakauer, J.W., 2009. Early imaging correlates of subsequent motor recovery after stroke. Ann. Neurol. 65, 596–602.
Martinez-Trujillo, J.C., Cheyne, D., Gaetz, W., Simine, E., Tsotsos, J.K., 2007. Activation of area MT/V5 and the right inferior parietal cortex during the discrimination of transient direction changes in translational motion. Cereb. Cortex 17, 1733–1739.
Mayka, M.A., Corcos, D.M., Leurgans, S.E., Vaillancourt, D.E., 2006. Three-dimensional locations and boundaries of motor and premotor cortices as defined by functional brain imaging: a meta-analysis. NeuroImage 31, 1453–1474.
Murase, N., Duque, J., Mazzocchio, R., Cohen, L.G., 2004. Influence of interhemispheric interactions on motor function in chronic stroke. Ann. Neurol. 55, 400–409.
Naik, S.K., Patten, C., Lodha, N., Coombes, S.A., Cauraugh, J.H., 2011. Force control deficits in chronic stroke: grip formation and release phases. Exp. Brain Res. 211, 1–15.
Nowak, D.A., Hermsdorfer, J., Topka, H., 2003. Deficits of predictive grip force control during object manipulation in acute stroke. J. Neurol. 250, 850–860.
Nowak, D.A., Grefkes, C., Dafotakis, M., Eickhoff, S., Kust, J., Karbe, H., Fink, G.R., 2008. Effects of low-frequency repetitive transcranial magnetic stimulation of the contralesional primary motor cortex on movement kinematics and neural activity in subcortical stroke. Arch. Neurol. 65, 741–747.
Paradis, A.L., Cornilleau-Peres, V., Droulez, J., Van De Moortele, P.F., Lobel, E., Berthoz, A., Le Bihan, D., Poline, J.B., 2000. Visual perception of motion and 3-D structure from motion: an fMRI study. Cereb. Cortex 10, 772–783.
Park, H.J., Furmaga, H., Cooperrider, J., Gale, J.T., Baker, K.B., Machado, A.G., 2015. Modulation of cortical motor evoked potential after stroke during electrical stimulation of the lateral cerebellar nucleus. Brain Stimul. 8, 1043–1048.
Patton, J.L., Stoykov, M.E., Kovic, M., Mussa-Ivaldi, F.A., 2006. Evaluation of robotic training forces that either enhance or reduce error in chronic hemiparetic stroke survivors. Exp. Brain Res. 168, 368–383.
Perez, M.A., Cohen, L.G., 2009. Scaling of motor cortical excitability during unimanual force generation. Cortex 45, 1065–1071.
Philip, B.A., Frey, S.H., 2014. Compensatory changes accompanying chronic forced use of the nondominant hand by unilateral amputees. J. Neurosci. Off. J. Soc. Neurosci. 34, 3622–3631.
Rabe, K., Livne, O., Gizewski, E.R., Aurich, V., Beck, A., Timmann, D., Donchin, O., 2009. Adaptation to visuomotor rotation and force field perturbation is correlated to different brain areas in patients with cerebellar degeneration. J. Neurophysiol. 101, 1961–1971.
Rehme, A.K., Eickhoff, S.B., Wang, L.E., Fink, G.R., Grefkes, C., 2011. Dynamic causal modeling of cortical activity from the acute to the chronic stage after stroke. NeuroImage 55, 1147–1158.
Rehme, A.K., Eickhoff, S.B., Rottschy, C., Fink, G.R., Grefkes, C., 2012. Activation likelihood estimation meta-analysis of motor-related neural activity after stroke. NeuroImage 59, 2771–2782.
Roitman, A.V., Pasalar, S., Ebner, T.J., 2009. Single trial coupling of Purkinje cell activity to speed and error signals during circular manual tracking. Exp. Brain Res. 192, 241–251.
Rose, D.K., Patten, C., McGuirk, T.E., Lu, X., Triggs, W.J., 2014. Does inhibitory repetitive transcranial magnetic stimulation augment functional task practice to improve arm recovery in chronic stroke? Stroke Res. Treat. 2014, 305236.
Sack, A.T., Kohler, A., Linden, D.E., Goebel, R., Muckli, L., 2006. The temporal characteristics of motion processing in hMT/V5 +: combining fMRI and neuronavigated TMS. NeuroImage 29, 1326–1335.
Samaei, A., Ehsani, F., Zoghi, M., Hafez Yosephi, M., Jaberzadeh, S., 2017. Online and offline effects of cerebellar transcranial direct current stimulation on motor learning in healthy older adults: a randomized double-blind sham-controlled study. Eur. J. Neurosci. 45 (9), 1177–1185.
Schaechter, J.D., Perdue, K.L., 2008. Enhanced cortical activation in the contralesional hemisphere of chronic stroke patients in response to motor skill challenge. Cereb. Cortex 18, 638–647.
Schmahmann, J.D., Doyon, J., McDonald, D., Holmes, C., Lavoie, K., Hurwitz, A.S., Kabani, N., Toga, A., Evans, A., Petrides, M., 1999. Three-dimensional MRI atlas of the human cerebellum in proportional stereotaxic space. NeuroImage 10, 233–260.

Serrien, D.J., Strens, L.H., Cassidy, M.J., Thompson, A.J., Brown, P., 2004. Functional significance of the ipsilateral hemisphere during movement of the affected hand after stroke. Exp. Neurol. 190, 425–432.
Smith, M.C., Stinear, C.M., 2016. Transcranial magnetic stimulation (TMS) in stroke: ready for clinical practice? J. Clin. Neurosci. 31, 10–14.
Spraker, M.B., Corcos, D.M., Kurani, A.S., Prodoehl, J., Swinnen, S.P., Vaillancourt, D.E., 2012. Specific cerebellar regions are related to force amplitude and rate of force development. NeuroImage 59, 1647–1656.
Stein, J.F., Glickstein, M., 1992. Role of the cerebellum in visual guidance of movement. Physiol. Rev. 72, 967–1017.
Stinear, C.M., Petoe, M.A., Byblow, W.D., 2015. Primary motor cortex excitability during recovery after stroke: implications for neuromodulation. Brain Stimul. 8, 1183–1190.
Takeuchi, N., Chuma, T., Matsuo, Y., Watanabe, I., Ikoma, K., 2005. Repetitive transcranial magnetic stimulation of contralesional primary motor cortex improves hand function after stroke. Stroke 36, 2681–2686.
Thach, W.T., Goodkin, H.P., Keating, J.G., 1992. The cerebellum and the adaptive coordination of movement. Annu. Rev. Neurosci. 15, 403–442.
Touvykine, B., Mansoori, B.K., Jean-Charles, L., Deffeyes, J., Quessy, S., Dancause, N., 2016. The effect of lesion size on the organization of the ipsilesional and contralesional motor cortex. Neurorehabil. Neural Repair 30 (3), 280–292.
Tunik, E., Saleh, S., Adamovich, S.V., 2013. Visuomotor discordance during visually-guided hand movement in virtual reality modulates sensorimotor cortical activity in healthy and hemiparetic subjects. IEEE Trans. Neural Syst. Rehabil. Eng. 21, 198–207.
Tzourio-Mazoyer, N., Landeau, B., Papathanassiou, D., Crivello, F., Etard, O., Delcroix, N., Mazoyer, B., Joliot, M., 2002. Automated anatomical labeling of activations in SPM using a macroscopic anatomical parcellation of the MNI MRI single-subject brain. NeuroImage 15, 273–289.
Vaillancourt, D.E., Thulborn, K.R., Corcos, D.M., 2003. Neural basis for the processes that underlie visually guided and internally guided force control in humans. J. Neurophysiol. 90, 3330–3340.
Vaillancourt, D.E., Mayka, M.A., Corcos, D.M., 2006. Intermittent visuomotor processing in the human cerebellum, parietal cortex, and premotor cortex. J. Neurophysiol. 95, 922–931.
Van Donkelaar, P., Lee, J.H., Drew, A.S., 2000. Transcranial magnetic stimulation disrupts eye-hand interactions in the posterior parietal cortex. J. Neurophysiol. 84, 1677–1680.
van Eimeren, T., Wolbers, T., Münchau, A., Büchel, C., Weiller, C., Roman Siebner, H., 2006. Implementation of visuospatial cues in response selection. NeuroImage 29, 286–294.
Verstynen, T., Diedrichsen, J., Albert, N., Aparicio, P., Ivry, R.B., 2005. Ipsilateral motor cortex activity during unimanual hand movements relates to task complexity. J. Neurophysiol. 93, 1209–1222.
Volz, L.J., Vollmer, M., Michely, J., Fink, G.R., Rothwell, J.C., Grefkes, C., 2017. Time-dependent functional role of the contralesional motor cortex after stroke. Neuroimage Clin. 16, 165–174.
Ward, N.S., Brown, M.M., Thompson, A.J., Frackowiak, R.S., 2003a. Neural correlates of motor recovery after stroke: a longitudinal fMRI study. Brain J. Neurol. 126, 2476–2496.
Ward, N.S., Brown, M.M., Thompson, A.J., Frackowiak, R.S., 2003b. Neural correlates of outcome after stroke: a cross-sectional fMRI study. Brain J. Neurol. 126, 1430–1448.
Ward, N.S., Brown, M.M., Thompson, A.J., Frackowiak, R.S., 2004. The influence of time after stroke on brain activations during a motor task. Ann. Neurol. 55, 829–834.
Weiller, C., Ramsay, S.C., Wise, R.J., Friston, K.J., Frackowiak, R.S., 1993. Individual patterns of functional reorganization in the human cerebral cortex after capsular infarction. Ann. Neurol. 33, 181–189.
Westerveld, A.J., Schouten, A.C., Veltink, P.H., van der Kooij, H., 2013. Control of thumb force using surface functional electrical stimulation and muscle load sharing. J. Neuroeng. Rehabil. 10, 104.
Wise, S.P., Boussaoud, D., Johnson, P.B., Caminiti, R., 1997. Premotor and parietal cortex: corticocortical connectivity and combinatorial computations. Annu. Rev. Neurosci. 20, 25–42.